



## CONSTRAINED LAYER DAMPING IN FINITE SHEARING DEFORMATIONS

JANG-HORNG YU AND R. C. BATRA

*Department of Engineering Science and Mechanics, M/C 0219, Virginia Polytechnic Institute and State University, Blacksburg, VA 24061, U.S.A.*

(Received 10 May 1999)

We analyze the damping induced by a homogeneous and isotropic viscoelastic layer embedded between a rigid solid cylinder of radius  $r_1$  and a homogeneous and isotropic elastic hollow cylinder of inner and outer radii  $r_2$  and  $r_3$  respectively. The composite cylinder is deformed by holding the inner cylinder fixed and applying a periodic displacement  $A = A_0 \sin \omega t$  to the outermost cylindrical surface. We assume that the length of the cylinder is very large as compared to  $r_3$ . Thus, the deformations are assumed to be functions of the radial co-ordinate  $r$  and time  $t$ . We use a set of orthonormal cylindrical basis vectors to describe deformations of the viscoelastic and elastic layers which are presumed to be made of incompressible materials. Also, the effect of inertia forces has been assumed to be negligible.

In the absence of body forces, quasistatic deformations of the viscoelastic and elastic layers are governed by the following equations expressing the balance of linear momentum:

$$\frac{\partial T_{rr}}{\partial r} + \frac{T_{rr} - T_{\theta\theta}}{r} = 0, \quad \frac{\partial T_{r\theta}}{\partial r} + \frac{2}{r} T_{r\theta} = 0. \quad (1)$$

Here,  $\mathbf{T}$  is the Cauchy stress tensor, and  $T_{rr}$ ,  $T_{\theta\theta}$ , and  $T_{r\theta}$  its physical components in the cylindrical co-ordinate system. The pertinent boundary and interface conditions are

$$T_{rr}^e(r_2, t) = T_{rr}^v(r_2, t), \quad T_{r\theta}^e(r_2, t) = T_{r\theta}^v(r_2, t), \quad \mathbf{u}^e(r_2, t) = \mathbf{u}^v(r_2, t),$$

$$T_{rr}^e(r_3, t) = 0, \quad u_\theta(r_3, t) = r_3 A_0 \sin \omega t, \quad u_r(r_1, t) = u_\theta(r_1, t) = 0. \quad (2)$$

Superscripts  $e$  and  $v$  signify quantities for the elastic and viscoelastic layers respectively. Equations (2)<sub>1</sub>, (2)<sub>2</sub> and (2)<sub>3</sub> guarantee the continuity of surface tractions and displacements across the viscoelastic/elastic layer interface. Similarly, equations (2)<sub>6-7</sub> ensure that the viscoelastic layer is perfectly bonded to the inner stationary rigid cylinder. Equations (2)<sub>4</sub> and (2)<sub>5</sub> imply that the normal tractions

vanish on the outermost cylindrical surface  $r = r_3$  and tangential displacements  $u_\theta$  are prescribed on it.

Equations (1) and (2) are supplemented by the following constitutive relations for the elastic and viscoelastic layers:

$$\mathbf{T}^e = -p_1(r, t)\mathbf{1} + \beta_1\mathbf{B},$$

$$\mathbf{T}^v = -p_2(r, t)\mathbf{1} + \beta_2\mathbf{B} - \frac{\Phi_0}{\gamma} \int_{-\infty}^t e^{-(t-\tau)/\gamma} \mathbf{E}_t(\tau) d\tau. \quad (3)$$

Here,  $\beta_1$  and  $\beta_2$  are constants,  $p_1$  and  $p_2$  hydrostatic pressure fields in the elastic and viscoelastic layers, respectively,  $\Phi_0$  is an instantaneous elastic modulus,  $\gamma$  is the relaxation time,  $\mathbf{B}$  the left Cauchy–Green tensor and  $\mathbf{E}_t(\tau)$  the relative Green–St Venant strain tensor. Note that  $\beta_1$  equals the shear modulus at zero strain for the elastic layer, and  $p_1$  and  $p_2$  are generally non-zero in the stress-free reference configurations of the elastic and viscoelastic layers. We note that

$$\mathbf{B} = \mathbf{F}\mathbf{F}^T, \quad \mathbf{E}_t(\tau) = \frac{1}{2}(\mathbf{F}_t^T(t)\mathbf{F}_t(\tau) - \mathbf{1}), \quad (4)$$

where  $\mathbf{F}$  is the deformation gradient,  $\mathbf{F}_t(\tau)$  the relative deformation gradient, and  $\mathbf{1}$  is the identity tensor. Equation (3)<sub>1</sub> implies that the elastic layer is made of a Mooney material (see e.g., Truesdell and Noll [1]), and the constitutive relation (3)<sub>2</sub> for the viscoelastic layer is taken from the Fosdick and Yu's paper [2].

We assume that the deformation field in the two layers is given by

$$r = R, \quad \theta = \Theta + f(r, t), \quad (5)$$

where  $\{r, \theta\}$  are the co-ordinates in the present configuration of the material point that occupied the place  $\{R, \Theta\}$  in the reference configuration. The physical components of the deformation gradient, the left Cauchy–Green strain tensor, and the relative Green–St Venant strain tensor are

$$\mathbf{F} = \begin{bmatrix} 1 & 0 \\ r \frac{\partial f(r, t)}{\partial r} & 1 \end{bmatrix}, \quad \mathbf{B} = \mathbf{F}\mathbf{F}^T = \begin{bmatrix} 1 & r \frac{\partial f(r, t)}{\partial r} \\ r \frac{\partial f(r, t)}{\partial r} & 1 + \left(r \frac{\partial f(r, t)}{\partial r}\right)^2 \end{bmatrix}, \quad (6, 7)$$

and

$$\mathbf{E}_t(\tau) = \frac{1}{2} \begin{bmatrix} r^2 \left( \frac{\partial f(r, \tau)}{\partial r} - \frac{\partial f(r, t)}{\partial r} \right)^2 & r \left( \frac{\partial f(r, \tau)}{\partial r} - \frac{\partial f(r, t)}{\partial r} \right) \\ r \left( \frac{\partial f(r, \tau)}{\partial r} - \frac{\partial f(r, t)}{\partial r} \right) & 0 \end{bmatrix}. \quad (8)$$

We now conclude from equations (3)–(5), (2)<sub>7</sub>, and (2)<sub>5</sub> that

$$f(r, t) = \frac{(A_0 \sin \omega t)r_3^2 - \kappa(t)r_2^2}{r_3^2 - r_2^2} - \frac{(A_0 \sin \omega t - \kappa(t))r_3^2 r_2^2}{r^2(r_3^2 - r_2^2)}, \quad r_2 \leq r \leq r_3, \quad (9)$$

$$f(r, t) = \frac{\kappa(t)r_2^2}{r_2^2 - r_1^2} \left(1 - \frac{r_1^2}{r^2}\right), \quad r_1 \leq r \leq r_2 \quad (10)$$

where  $\kappa(t) = f(r_2, t)$  describes the angular displacement of a point on the interface between the two layers. Equations (3)–(5), and (2)<sub>2</sub> yield

$$\frac{2\beta_1 r_3^2 (A_0 \sin \omega t - \kappa(t))}{r_3^2 - r_2^2} = \frac{2\beta_2 r_1^2 \kappa(t)}{r_2^2 - r_1^2} - \frac{\Phi_0 r_1^2}{r_2^2 - r_1^2} \int_{-\infty}^t \frac{e^{-(t-\tau)/\gamma}}{\gamma} ((\kappa(\tau) - \kappa(t))) d\tau. \quad (11)$$

In order to solve this integral equation, we introduce an auxiliary variable,

$$\zeta \equiv \int_{-\infty}^t \frac{e^{-(t-\tau)/\gamma}}{\gamma} (\kappa(\tau) - \kappa(t)) d\tau, \quad (12)$$

and note that

$$\dot{\zeta} = -\frac{1}{\gamma} \zeta - \dot{\kappa} \quad (13)$$

where  $\dot{\zeta} = d\zeta/dt$ . Thus, equation (11) can be written as

$$(\eta_1 + \eta_2)\kappa(t) - \eta_3 \zeta(t) = \eta_1 A_0 \sin \omega t, \quad (14)$$

where

$$\eta_1 = \frac{2\beta_1 r_3^2}{r_3^2 - r_2^2}, \quad \eta_2 = \frac{2\beta_2 r_1^2}{r_2^2 - r_1^2}, \quad \eta_3 = \frac{\Phi_0 r_1^2}{r_2^2 - r_1^2}. \quad (15)$$

The elimination of  $\zeta$  from equations (13) and (14) results in the ordinary differential equation

$$\gamma(\eta_1 + \eta_2 + \eta_3)\dot{\kappa}(t) + (\eta_1 + \eta_2)\kappa(t) = \gamma\omega\eta_1 A_0 \cos \omega t + \eta_1 A_0 \sin \omega t, \quad (16)$$

whose solution is

$$\frac{\kappa(t)}{A_0} =$$

$$\frac{\eta_1 \eta_3 \gamma \omega e^{-(\eta_1 + \eta_2)t/(\eta_1 + \eta_2 + \eta_3)\gamma} - \eta_1 \eta_3 \gamma \omega \cos(\omega t) + \eta_1 [(\eta_1 + \eta_2) + \gamma^2 \omega^2 (\eta_1 + \eta_2 + \eta_3)^2] \sin(\omega t)}{(\eta_1 + \eta_2)^2 + \gamma^2 \omega^2 (\eta_1 + \eta_2 + \eta_3)^2}$$

From equation (3), we see that the shear stress in the composite cylinder is given by

$$T_{r\theta}^e = \frac{2\beta_1(A_0 \sin \omega t - \kappa(t))r_3^2 r_2^2}{r^2(r_3^2 - r_2^2)}, \quad r_2 \leq r \leq r_3, \quad (18)$$

$$T_{r\theta}^v = \frac{2\beta_2 \kappa(t) r_1^2 r_2^2}{r^2(r_2^2 - r_1^2)} - \frac{\Phi_0 r_1^2 r_2^2}{r^2(r_2^2 - r_1^2)} \int_{-\infty}^t \frac{e^{-(t-\tau)/\gamma}}{\gamma} (\kappa(\tau) - \kappa(t)) d\tau, \quad r_1 \leq r \leq r_2, \quad (19)$$

and it satisfies the equilibrium equation (1)<sub>2</sub>. For the deformation field (5), damping is induced only by the shear stress  $T_{r\theta}$ . Therefore, we omit finding normal stresses and pressure fields from equation (1)<sub>1</sub> and the pertinent boundary condition in equation (2). The energy dissipated,  $\Delta$ , per unit length of the cylinder in a cycle equals the work done by the viscous part of the stress in equation (3)<sub>2</sub>. That is,

$$\Delta = \int_0^{2\pi/\omega} \int_{r_1}^{r_2} \text{tr}(T_d^v D) 2\pi r dr dt, \quad (20)$$

where  $T_d^v$  equals the third term on the right-hand side of equation (3)<sub>2</sub> and  $D$  is the strain-rate tensor defined by

$$D = \frac{1}{2}(\dot{F}F^{-1} + F^{-1T}\dot{F}^T). \quad (21)$$

Unless otherwise specified, numerical results have been computed by setting  $\omega = 0.1$ ,  $A_0 = 1$ ,  $r_1 = 1.0$ ,  $r_3 = 5$ ,  $\Phi_0/\beta_1 = \beta_2/\beta_1 = 0.1$ . The results presented below are in terms of the non-dimensional energy

$$\Delta_n = \frac{\Delta}{2\pi r_1^2 \beta_1}, \quad (22)$$

dissipated per cycle.

Figure 1 depicts, for  $r_2 = 2, 3$  and  $4$ , the angular displacement field  $f(r, t)$  and the shear stress  $T_{r\theta}$  at  $t = 5\pi$  when the applied tangential displacement is maximum, and at  $t = 10\pi$  when the applied tangential displacement is zero. At  $t = 5\pi$ , we see that the amplitude of the motion of the interface decreases with a decrease in the thickness of the viscoelastic layer implying thereby that a higher percentage of the prescribed tangential displacement is taken up by the elastic layer as the viscoelastic layer becomes thinner. The corresponding maximum shear stress is also higher for a thinner viscoelastic layer. Due to the material relaxation, at  $t = 10\pi$  we see that the “residual” angular displacement of the interface is higher for the thinner viscoelastic layer, and the magnitude of the shear stress at the viscoelastic layer/rigid cylinder interface increases slowly with a decrease in the thickness of the viscoelastic layer.

Figure 2 exhibits the angular displacement field  $f(r, t)$  for  $r_2 = 3$  and  $t = 5\pi$  and  $10\pi$  for  $\gamma = 1, 5$  and  $10$ . The computed values of  $\kappa(t) = f(3, t)$  for different values of

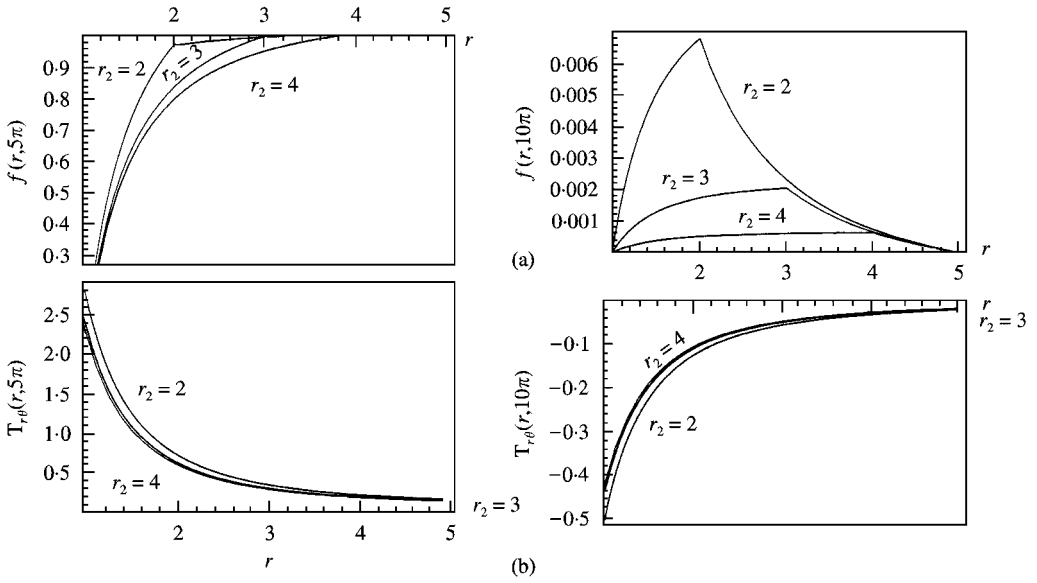


Figure 1. Deformation field  $f(r, t)$  and (b) shear stress  $T_{r\theta}$  versus  $r$  for different thicknesses of the viscoelastic layer ( $\gamma = 10$ ).

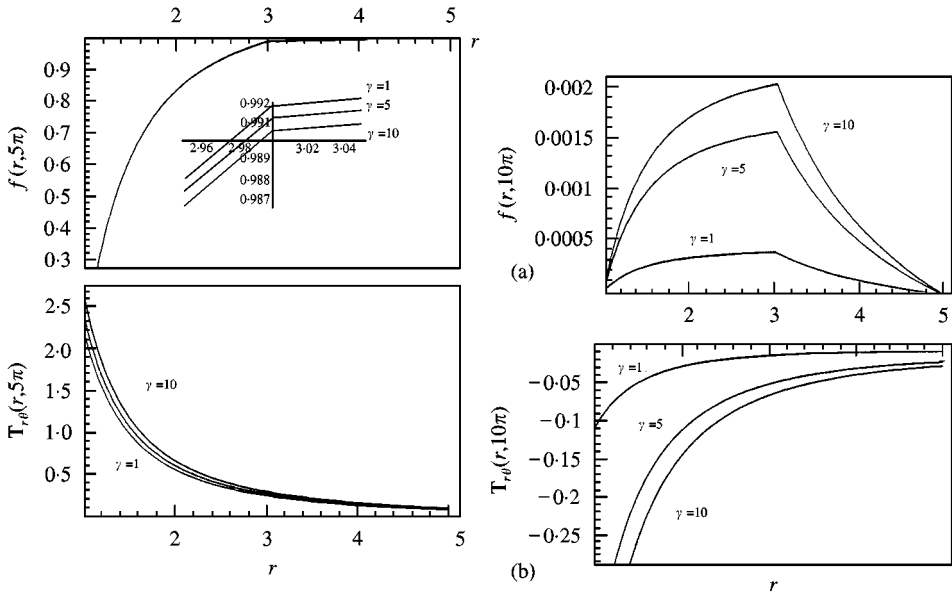


Figure 2. Deformation field  $f(r, t)$  and (b) shear stress  $T_{r\theta}$  versus  $r$  for different values of the material relaxation time ( $r_2 = 3$ ).

the relaxation time,  $\gamma$ , revealed that the values of  $\kappa(5\pi)$  are not affected much by the value of  $\gamma$ . However, at  $t = 10\pi$ , the angular displacement of the interface is larger for the material that takes longer to relax. This is also true for the values of the shear stress.

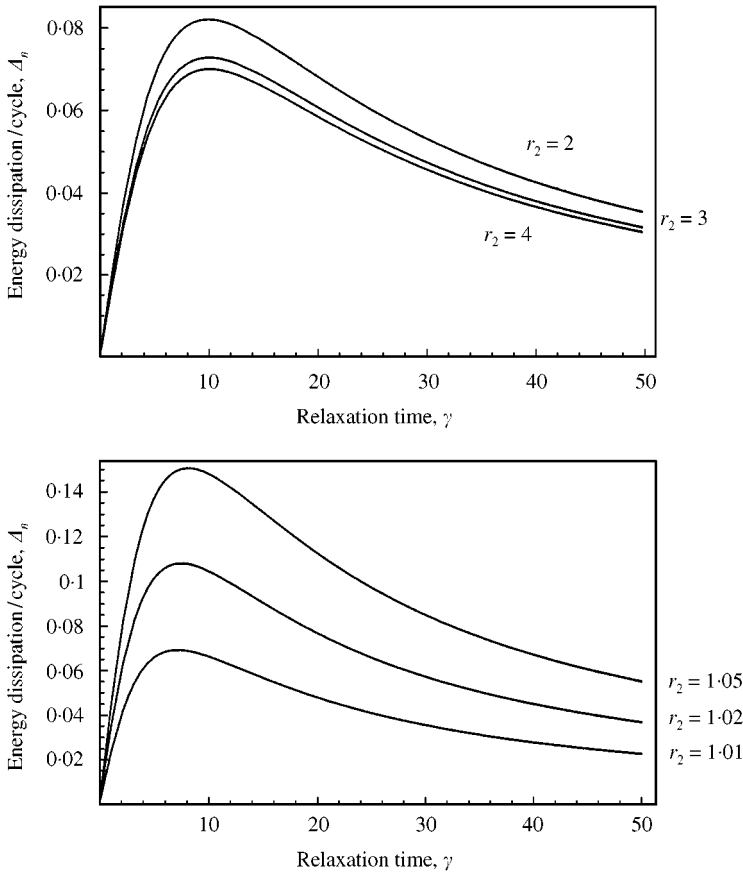


Figure 3. Energy loss per cycle,  $\Delta_n$ , as a function of the relaxation time  $\gamma$  for different thicknesses of the viscoelastic layer.

Figure 3 shows, for different layer thicknesses, the energy dissipated per cycle versus the relaxation time,  $\gamma$ . We see that the value of  $\gamma$  significantly affects the energy dissipated per cycle. For the fixed radius of the inner solid cylinder and the fixed outer radius of the outer elastic cylinder, the energy dissipated/cycle first increases with an increase in the thickness of the viscoelastic layer and then decreases implying thereby that an optimum thickness of the viscoelastic layer results in the maximum energy dissipated/cycle. Our calculations show that the energy dissipation is maximum when  $r_2 \approx 1.06$ .

Figure 4 evinces the effect of the inner radius on the damping effect of the constrained layer. Here, we choose the values  $r_1 = 1, 10, 100$  and keep the values  $r_2 - r_1 = r_3 - r_2 = 2$ .

Figure 5 exhibits the energy dissipation as a function of  $\gamma$  for three values, namely, 0.1, 0.5, and 1.0 of  $\Phi_0/\beta_1$ . We see that the energy dissipation first increases, reaches a plateau and then decreases with an increase in the value of the relaxation time. Results plotted in Figure 5 suggest that  $\Delta_n$  is maximum when  $\gamma \approx (\eta_1 + \eta_2)/\omega(\eta_1 + \eta_2 + \eta_3)$ . Therefore, for optimum damping the value of

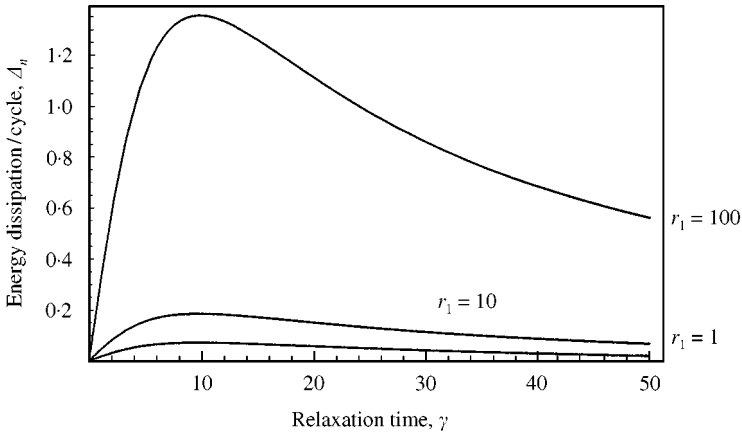


Figure 4. Energy loss per cycle,  $\Delta_n$ , as a function of the relaxation time  $\gamma$  for different values of the inner radius.

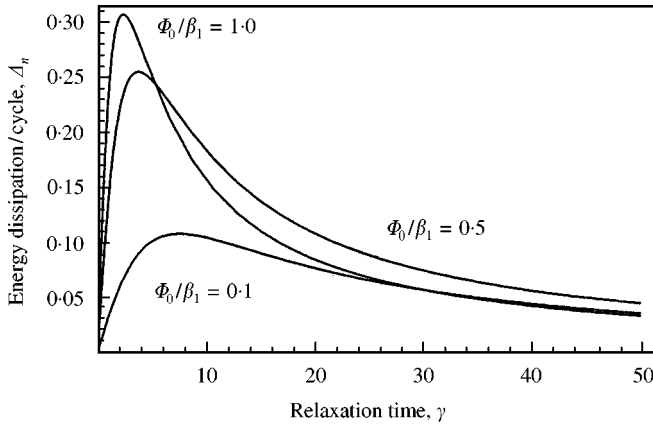


Figure 5. Energy loss per cycle,  $\Delta_n$ , as a function of the relaxation time  $\gamma$  for three different values of  $\Phi_0/\beta_1$  ( $r_2 = 1.02$ ).

$\gamma$  decreases with an increase in the value of  $\Phi_0/\beta_1$ . For twisting of a homogeneous and isotropic viscoelastic cylinder, Batra and Yu [3] found that the energy dissipated per cycle is maximum when  $\gamma = 1/\omega$ . Thus, for shearing deformations of the constrained layer, the elastic modulus and the thickness of the bounding layer affect the energy dissipated in the viscoelastic layer.

We note that the aforegiven procedure can be used to analyze finite shearing deformations of a composite cylinder made of different viscoelastic layers.

#### ACKNOWLEDGMENT

This work was supported by the ARO grant DAAG 55-98-1-0030 to Virginia Polytechnic Institute and State University. JHY would like to thank Drs S.S. Vel, Li Chen, and Z. Cheng for their constructive comments.

## REFERENCES

1. C. TRUESDELL and W. NOLL 1965 *Handbook of Physics*, Vol. III/3. New York: Springer. The non-linear field theories of mechanics.
2. R. L. FOSDICK and J. H. YU 1998 *International Journal of Non-linear Mechanics* **33**, 165–188. Thermodynamics, stability and non-linear oscillations of viscoelastic solids—II. History type solids.
3. R. C. BATRA and J. H. YU 1999 Torsion of a viscoelastic cylinder. submitted for publication.